NASA TECHNICAL NOTE

NASA TN D-3125

A NEW APPROACH TO THE EXPLANATION OF THE FLUTTER MECHANISM

by Mario H. Rheinfurth and Fredrick W. Swift

George C. Marshall Space Flight Center
Huntsville, Ala.

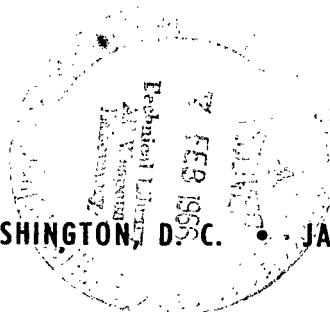NATIONAL AERONAUTICS AND SPACE ADMINISTRATION • WASHINGTON, D.C. • JANUARY 1966

A NEW APPROACH TO THE EXPLANATION

OF THE FLUTTER MECHANISM

By Mario H. Rheinfurth and Fredrick W. Swift

George C. Marshall Space Flight Center
Huntsville, Ala.

TABLE OF CONTENTS

LIST OF ILLUSTRATIONS

DEFINITION OF SYMBOLS

Symbol   Definition

Symbol	Definition
S	Plan area of typical section
g	Dynamic pressure $1/2\,\rho\,V^2$
V	Air Speed
I	Moment of inertia about C.M.
ω_1	Uncoupled bending frequency
ω_2	Uncoupled torsional frequency
k_{12}, k_{21}	Static structural coupling terms
ω_h	Coupled bending frequency
ω_α	Coupled torsional frequency
$\overline{X}_P$	Location of aerodynamic center
$\overline{X}_E$	Location of elastic axis
m	Mass of wing
C_1	Damping coefficient of bending mode
C_2	Damping coefficient of torsion mode
σ_1	Decay rate of bending mode
σ_2	Decay rate of torsion mode
C_L	Lift coefficient
α	Rotational displacement
y	Lateral displacement
k_1	Bending spring constant
k_2	Torsion spring constant

DEFINITION OF SYMBOLS (Concluded)

Symbol	Definition
L	Aerodynamic lift force
r	Radius of gyration about C.M.
M	Aerodynamic moment
s	Laplace transform variable
K	Aerodynamic feedback parameter

Other symbols and abbreviations are explained in the text.

A NEW APPROACH TO THE EXPLANATION OF THE FLUTTER MECHANISM

SUMMARY

The paper demonstrates the feasibility and effectiveness of analyzing the stability behavior of a simplified bending-torsion flutter model by the root-locus method of W. R. Evans. This method promotes an intuitive physical interpretation of the flutter mechanism by exposing its intrinsic feedback principle, and lends itself to a systematic and complete classification of the stability patterns of the system by enumerating all possible pole-zero constellations in the complex plane. Results of corresponding conventional studies using Routh-Hurwitz stability criteria are quickly verified and extended. The inclusion of structural damping in the analysis sheds new light on long standing questions about the effect of energy dissipation on system stability and reveals its extreme sensitivity to damping parameter variations. The paper concludes with a discussion of the potentials and limitations of the root-locus method for preliminary design studies and flutter analyses of systems with many degrees of freedom.

I. INTRODUCTION

Theoretical investigations of the flutter phenomenon started during the latter part of World War I after the first flutter incidents became known. The subsequent years were marked by concentrated efforts to develop a rigorous mathematical theory of unsteady aerodynamics, which was considered the principal agent responsible for the dynamic aeroelastic instability encountered in flutter. With increasing mathematical complexity of the unsteady aerodynamic theory, however, the real origin of the flutter mechanism became progressively concealed. Although it was understood that a physical rather than mathematical understanding of the flutter mechanism could be brought about only through a simplified flutter model, most researchers felt that discarding the unsteady portion of the aerodynamics would destroy the essentially dynamic features of the flutter phenomenon. In fact, it was known for many years that the source of the flutter mechanism of a purely rotational motion of a typical wing section is represented by the nonstationary component of the aerodynamic moment acting on the wing.

Guided by a discussion of a simplified control surface flutter model in a classical textbook by von Karman (Ref. 1), several analysts were also able to demonstrate, however, that an apposite bending-torsion flutter model could be established by using only static aerodynamics as a forcing function (Refs. 2 and 3). This system proved not only

to be simple enough to promote a clear physical understanding of the flutter mechanism but also revealed surprisingly good agreement with experimental flutter tests for a large number of wing configurations.

The authors of these studies analyze the stability behavior of the system by applying the classical Routh-Hurwitz stability criteria. Although relatively simple, this technique still leads to rather cumbersome expressions from which the influence of parameter changes on system stability has to be assessed. The present study presents a simpler approach of systems analysis by rearranging the characteristic polynomial in order to uncover the intrinsic feedback principle of the flutter mechanism. As a direct consequence of this rearrangement, it is possible to analyze the system stability by using the root locus method of control system design originated by W. R. Evans (Ref. 4). This technique provides an instantaneous and complete appraisal of the effect of parameter changes on the stability of the system by simple inspection of its pole-zero constellation in the complex s-plane. Results of previous studies can then readily be verified as well as extended.

II. TWO-DEGREE-OF-FREEDOM FLUTTER MODEL

Since the main objective of the present study is to expose a new technique of analyzing system stability and to compare it with previous analyses, we select the same simplified bending-torsion flutter model already investigated by previous authors. The typical wing section and pertinent system parameters of this flutter model are shown in Figure 1. The origin of the coordinate system shall be located at the equilibrium position of the center of mass of the model. The structural damping of the system is accounted for by an equivalent viscous damping law.

To derive the equations of motion in bending and torsion, we sum all forces positive upwards and moments positive in the clockwise direction.

This yields the bending motion as

$$m\ddot{y} + C_1 \dot{y} + k_1 (y - \overline{X}_E \alpha) = L \tag{1}$$

and the torsional motion as

$$I \ddot{\alpha} + C_2 \dot{\alpha} + k_2 \alpha - k_1 \overline{X}_E (y - \overline{X}_E \alpha) = M \ . \tag{2}$$

For the aerodynamic operator we employ quasi-steady aerodynamics intended to be used for a later discussion of the effect of aerodynamic energy dissipation on system stability. Thus, the aerodynamic force and moment on the right hand side of equations (1) and (2) are assumed to be proportional to the instantaneous angle of attack at the center of mass of the flutter model, i.e.,

2

$$L = q S \frac{\partial C_L}{\partial \alpha} \left(\alpha - \frac{\dot{y}}{V} \right) \tag{3}$$

$$M = -q S \overline{X}_P \frac{\partial C_L}{\partial \alpha} \left(\alpha - \frac{\dot{y}}{V} \right) \quad . \tag{4}$$

For convenience of the subsequent analysis, we furthermore introduce the following abbreviations:

$$\omega_1^2 = \frac{k_1}{m} \quad ; \quad \omega_2^2 = \frac{\overline{X}_E^2 k_1 + k_2}{I} \quad ; \quad k_{12} = \omega_1^2 \overline{X}_E \quad ;$$

$$k_{21} = \frac{\omega_1^2 \overline{X}_E m}{I} \quad ; \quad \sigma_1 = \frac{C_1}{2m} \quad ; \quad \sigma_2 = \frac{C_2}{2I} \quad : \quad N' = q S \frac{\partial C_L}{\partial \alpha} \quad .$$

The equations of motion can now be written in the form:

$$\ddot{y} + \left(2\sigma_1 + \frac{N'}{mV} \right) \dot{y} + \omega_1^2 y - \left(k_{12} + \frac{N'}{m} \right) \alpha = 0 \tag{5}$$

$$\ddot{\alpha} + 2\sigma_2 \dot{\alpha} + \left(\omega_2^2 + \frac{N'\overline{X}_P}{I} \right) \alpha - k_{21} y - \frac{N'\overline{X}_P}{IV} \dot{y} = 0 \quad . \tag{6}$$

The characteristic polynomial of this set of homogeneous differential equations with constant coefficients is of fourth order in the Laplace transform variable s and reads:

$$s^4 + \left(2\sigma_1 + 2\sigma_2 + \frac{N'}{mV} \right) s^3 + \left(\omega_1^2 + \omega_2^2 + \frac{N'\overline{X}_P}{I} + 4\sigma_1\sigma_2 \right.$$

$$\left. + 2\sigma_2 \frac{N'}{mV} \right) s^2 + \left[\left(2\sigma_1 + \frac{N'}{mV} \right) \left(\omega_2^2 + \frac{N'\overline{X}_P}{I} \right) + 2\omega_1^2 \sigma_2 \right. \tag{7}$$

$$\left. - \left(k_{21} + \frac{N'}{m} \right) \frac{N'\overline{X}_P}{IV} \right] s - k_{21} \left(k_{12} + \frac{N'}{m} \right) + \omega_1^2 \left(\omega_2^2 + \frac{N'\overline{X}_P}{I} \right) = 0 \quad .$$

In order to study the effect of the aerodynamics of the system stability by the root locus method, we have to separate the aerodynamic operator from the structural parameters of the system. As a result the characteristic polynomial appears in the form:

3

$$s^4 + 2(\sigma_1 + \sigma_2) \ s^3 + (4\sigma_1\sigma_2 + \omega_1^2 + \omega_2^2) \ s^2 + 2(\sigma_1\omega_2^2 + \sigma_2\omega_1^2) \ s$$

$$+ (\omega_1^2\omega_2^2 - k_{12}k_{21}) + \frac{N'\overline{X}_P}{I} \left[\frac{I \, s^3}{mV\widetilde{X}_P} + \left(1 + \frac{2\sigma_2 I}{mV\widetilde{X}_P}\right) \ s^2 \right.$$

$$\left. + \left(2\sigma_1 - \frac{\omega_1^2\overline{X}_E}{V\overline{X}_P}\right) s + \omega_1^2 \left(1 - \overline{X}_E \Big/ \overline{X}_P\right)\right] = 0 \ . \tag{8}$$

We are now ready to analyze the stability of the system. However, since the aeroelastician does not often encounter problems which call for application of the root locus method, it would be appropriate first to discuss briefly some of its basic principles and rules.

III. THE ROOT LOCUS METHOD

The root locus method has application in problems which call for analyzing the effect of a parameter K on the roots of a polynomial which is composed of two additive parts in the form:

$$P(s) = M(s) + K \, N(s) = 0 \tag{9}$$

where $M(s)$ and $N(s)$ represent polynomial in s whose coefficients are usually assumed to be real.

The usefulness of the root locus method in analyzing such problems lies in the simplicity with which the effect of a change in the parameter K can be appraised. Its rules for constructing the root loci as a function of K involve both analytical and graphical concepts. There exists a wide variety of special rules which are often tailored to the particular needs of the problem under investigation. Only those rules pertinent for the subsequent discussion will be listed here. Others can be found in standard textbooks on classical control theory (e.g., Ref. 5). The first step of the root locus method consists of factorizing the polynomials $M(s)$ and $N(s)$ of equation (9) which results in the standard form

$$G(s) = \frac{N(s)}{M(s)} = \frac{(s - z_1) \ (s - z_2) \cdots (s - z_n)}{(s - P_1) \ (s - P_2) \cdots (s - P_m)} = -\frac{1}{K} \ . \tag{10}$$

The parameter K (real or complex) is often referred to as "loop gain" and $G(s)$ as the (open-loop), "transfer function" of the system. This terminology stems from the principal application of the root locus method in feedback control systems. The solution of equation (10) is called a root whose location in the complex s-plane depends

on K such that $S = S(K)$. In this respect we can consider the root locus a conformal mapping of the (complex) K-plane into the complex s-plane. The number of separate root loci, of course, equals the order of the original polynomial $P(s)$.

The essence of the root locus method now consists in representing the expression (10) in polar form. This can be done graphically, as in Figure 2, by representing the transfer function $G(s)$ in terms of vectors originating at the various poles and zeros and terminating at the point s. Analytically, each vector is described by a complex number defined by magnitude and angle such that

$$\vec{A} = |A| \, e^{j\varphi_A} \tag{11}$$

Thus, equation (10) can also be written as:

$$\frac{\vec{Z_1}\,\vec{Z_2} \cdots \vec{Z_n}}{\vec{P_1}\,\vec{P_2} \cdots \vec{P_m}} = \frac{\left(Z_1 e^{j\varphi_1}\right)\left(Z_2 e^{j\varphi_2}\right) \cdots \left(Z_n e^{j\varphi_n}\right)}{\left(P_1 e^{j\chi_1}\right)\left(P_2 e^{j\chi_2}\right) \cdots \left(P_m e^{j\chi_m}\right)} = -\frac{1}{K} \, . \tag{12}$$

For a point in the complex s-plane to be on a root locus, it has to satisfy two separate conditions: The <u>angle condition</u>

$$(\varphi_1 + \varphi_2 + \cdots \varphi_n) - (\chi_1 + \chi_2 + \cdots \chi_m) = \Theta \tag{13}$$

where Θ is the net angle of the (complex) right-hand side. As an example for real K, a point in the complex s-plane can only represent a root of the original polynomial $P(s)$ if the net angle from all vectors terminating at this point is either $180° \pm n360°$ ($K > 0$) or $0° \pm n\,360°$ ($K < 0$) where n is any integer.

The angle condition already contains all information necessary for constructing the root loci. Consequently, the majority of the rules of the root locus method can be derived from it. The gain K corresponding to a specific point on a root locus, however, has to be determined by the <u>magnitude condition</u>

$$|K| = \frac{P_1\,P_2 \cdots \cdots P_m}{Z_1 Z_2 \cdots \cdots Z_n} \, . \tag{14}$$

Although often of secondary importance, the magnitude condition furnishes the basic rule that the root loci originate at the poles of the transfer function for $K = 0$ and approach the zeros for $K = \infty$.

In the approximate construction of the root loci, one can take advantage of a force analogy. According to this the root locus is in the direction of the net vector force acting on a particle which is repelled from the poles and attracted by the zeros inversely proportional to their distances. For simple pole-zero configurations, it is possible to obtain an analytic expression for the root loci themselves. Such an analytic representation of the root locus is obtained by setting $s = \sigma + j\omega$ in the polynomials $M(s)$ and

N(s) of equation (9) and derive conditions which have to be satisfied by the resulting real and imaginary parts of equation (9). This technique affords some additional analytical rules concerning asymptotes, intersection of the root locus with the real or imaginary axis and other relationships (Ref. 6).

IV. PARAMETRIC STABILITY ANALYSIS

The characteristic polynomial of equation (8) is still rather complicated. However, as shown by previous analysts, it is possible to introduce further simplifications without eliminating the basic source leading to the dynamic instability or flutter. To this effect we omit for our first discussion all terms in equation (8) which represent aerodynamic and structural energy dissipation. The resulting characteristic polynomial is then biquadratic and can be written in the form amenable to the root locus method

$$\frac{(s^2 + \omega_n^2)}{s^4 + (\omega_1^2 + \omega_2^2) s^2 + (\omega_1^2 \omega_2^2 - k_{12} k_{21})} = -\frac{1}{K} \tag{15}$$

where the "loop gain" K represents the aerodynamic feedback coupling which exists between the two degrees of freedom of the system. Since $K = \dfrac{N'\overline{X}_P}{I}$ it is proportional to the angular acceleration which the wing experiences at its equilibrium caused by an aerodynamic moment acting on it. As such, K serves as a measure for the "turnability" of the wing. The feedback parameter K can be either positive or negative depending on the location of the aerodynamic center relative to the center of mass. If the aerodynamic center is aft of the center of mass, the aerodynamic coupling tends to oppose any deviation from the nominal position (equilibrium) of the wing and we speak of negative feedback. For a forward location of the aerodynamic center, however, the aerodynamic feedback coupling reinforces an initial disturbance and we speak of positive feedback. Intuitively the latter condition will exhibit a higher tendency towards instability than the former.

The four poles of the transfer function are seen to represent physically the undamped (structurally) coupled frequencies of the bending-torsion model as observed in a ground vibration test. They occur in conjugate pairs and lie on the imaginary axis of the complex s-plane:

$$\omega_\alpha^2, y = -\frac{\omega_1^2 + \omega_2^2}{2} \pm \sqrt{\frac{(\omega_1^2 + \omega_2^2)^2}{4} - (\omega_1^2 \omega_2^2 - k_{12} k_{21})} \ . \tag{16}$$

For unswept wings, the structural coupling between the bending and torsion mode is usually very small (Ref. 7). Mathematically speaking, this means that $\omega_2^2/\omega_1^2 >> \overline{X}_E^2/r^2$.

In view of the approximations made for the present discussion, therefore, it is not necessary to distinguish between the uncoupled and (structurally) coupled frequencies of the

system. This simplification is not at all serious and can easily be waived to refine the analysis or extend it to sweptback wings which display pronounced interaction between the various modes.

The location of the two zeros of the transfer function is determined by

$$\omega_0{}^2 = \omega_1{}^2 \left(1 - \frac{\overline{X}_E}{\overline{X}_P}\right) \tag{17}$$

and is, thus, a function of the bending mode frequency and the ratio of the location of elastic axis and aerodynamic center relative to the center of mass of the model, but independent of the torsional frequency. For positive $\omega_0{}^2$ they lie on the imaginary axis; for negative $\omega_0{}^2$, on the real axis of the complex s-plane. Due to the symmetry of the pole-zero constellation of the transfer function, we can identify four different pole-zero topologies. They are depicted in Figure 3. As mentioned above, the feedback parameter K can assume both positive and negative values. Consequently, we arrive at two sets of root loci, one for positive K ($\overline{X}_P > 0$) where the net angle of the vectors add up to 180° and one for negative K ($\overline{X}_P < 0$) where the net angle is zero. Each set comprises four different pole-zero constellations. The resulting eight stability patterns exhaust all possible parameter variations. Their codification is extremely simple (shown in Figures 4 and 5). In these figures the root loci are portrayed only approximately and only for the upper half-plane; the lower half-plane is symmetric to the real axis. It can be easily verified that the hatched portions of the real and imaginary axis represent admissible locations for roots of the characteristic polynomial because they satisfy one of the above mentioned angle requirements. Once these portions are identified, one can quickly complete the missing sections of the root loci, at least in their qualitative shape. The direction in which the root locus is traversed follows from the magnitude condition of the root locus method. In addition to the root loci, Figures 4 and 5 show in the left column the parameter condition leading to the particular pole-zero constellation and in the right column the dependency of the aerodynamically coupled frequencies of the system on the feedback parameter K. The pattern of these frequency characteristics unfolds at once from the adjacent root loci. Although the situation is nearly self-explanatory, it seems opportune to direct attention to several important points:

(1)   Flutter can only occur if both frequencies approach each other with increasing airspeed.

(2)   No flutter is possible if both frequencies increase with increasing airspeed. In this case (A-2), the low-frequency mode asymptotically approaches a finite frequency.

(3)   A decrease in both frequencies always leads to divergence.

(4)   Flutter can be entered from below and above. In this case, the flutter frequency associated with the high airspeed lies outside the interval between the high and low frequency mode.

(5)   There exist three different flutter modes:

    a.   Flutter occurs at one airspeed only (B-4).

    b.   Flutter sets on at low airspeed and ceases after the high flutter speed is exceeded (A-1).

    c.   Flutter ceases after the high flutter speed is exceeded but the wing becomes divergently unstable with increasing airspeed (B-3-a).

It should be emphasized that these rules hold only for the simplified flutter model under investigation. Conclusions of the aeroelastic behavior of an actual wing have to be made with extreme care.

    Collecting all parameter conditions on the left column of Figures 4 and 5 leads to the aeroelastic stability criteria for the composite wing. They are illustrated in Figure 6 with the location of the elastic axis as the independent variable. As was expected, a wing with its aerodynamic center aft of the center of mass exhibits much less tendency toward instability than a wing with forward aerodynamic center. It is quite interesting to notice that a center of mass forward of the elastic axis no doubt prevents flutter, but is not a safeguard against divergence as has sometimes been stated. Since the majority of practical wing configurations lead to an aerodynamic center forward of the center of mass, the only way to prevent instability is to raise the critical airspeed above the expected operational flight range of the system.

    The critical airspeed or critical gain K at which instability sets on is easily derived from the magnitude condition given in equation (14). From this follows the flutter gains as:

$$K_F = \left| \frac{\left(\omega_F^2 - \omega_1^2\right)\left(\omega_F^2 - \omega_2^2\right)}{\left(\omega_F^2 - \omega_0^2\right)} \right| \tag{18}$$

and the divergence gain simply by setting $\omega_F = 0$ as:

$$K_D = \left| \frac{\omega_1^2 \, \omega_2^2}{\omega_0^2} \right| \tag{19}$$

Since all quantities in equation (19) are known, the divergence speed can be explicitly written down. For the torsional divergence speed $(\omega_2 > \omega_1)$, we find

$$V_T^2 = \frac{2 \, k_2}{\rho \, S \left| \overline{X}_P - \overline{X}_E \right| \frac{\partial C_L}{\partial \alpha}} \tag{20}$$

and for the flexural divergence speed $(\omega_2 < \omega_1)$, we find

8

$$V_B{}^2 = \frac{2 k_1}{\rho S \left| \overline{X}_P - \overline{X}_E \right| \left| \frac{\partial C_L}{\partial \alpha} \right|} \quad . \tag{21}$$

Since the flutter frequency ω_F appearing in equation (18) is unknown the expression for the flutter speed is more complicated. The unknown flutter frequency is determined by the points where the root locus breaks away from the imaginary axis. Using the above mentioned force analogy, they are found to be the equilibrium points of the force field created by the pole-zero constellation of the system. Accordingly, the flutter frequency is given by

$$\frac{1}{\omega_F{}^2 - \omega_1{}^2} + \frac{1}{\omega_F{}^2 - \omega_2{}^2} - \frac{1}{\omega_F{}^2 - \omega_0{}^2} = 0 \tag{22}$$

which leads to the biquadratic equation in $\omega_F{}^2$

$$\omega_F{}^4 - 2\omega_0{}^2\omega_F{}^2 + \omega_0{}^2 (\omega_1{}^2 + \omega_2{}^2) - \omega_1{}^2 \omega_2{}^2 = 0 \quad . \tag{23}$$

The four roots of this polynomial do not always represent flutter frequencies. The flutter mode B-4, for example, has only one flutter speed and consequently, only two roots of the polynomial have physical significance. The other two roots are imaginary and represent the arrival points of the root locus at the real axis. Because of these extraneous roots, the explicit expression for the flutter speed becomes awkward and difficult to interpret physically. To establish a clearer, although less precise, correlation between system parameters and flutter speed, some typical critical flutter and divergence gains were calculated and plotted in Figures 7 and 8. To preserve correspondence with Figure 6, the location of the elastic axis was again selected as independent variable.

The characteristic hyperbolic pattern of the critical gain curves suggests the possibility to delay flutter and divergence onset for all elastic axis locations by increasing the critical gains at their endpoints. According to the magnitude condition, the flutter gain at the endpoint of the flutter interval is given by

$$K_F = \left| \omega_1{}^2 - \omega_2{}^2 \right| \tag{24}$$

from which follows the corresponding flutter speed as

$$V_F{}^2 = \frac{2m r^2}{\rho \overline{X}_P S \frac{\partial C_L}{\partial \alpha}} \left| \omega_1{}^2 - \omega_2{}^2 \right| \quad . \tag{25}$$

9

Several interesting conclusions can be drawn from the situation at hand:

(1)   Critical gains are sensitive to elastic axis variations close to the center of mass. This calls for a conservative design philosophy for many practical configurations falling into this category.

(2)   Decreasing density ratio lowers the flutter speed. This is in agreement with classical flutter analyses for high density ratios but at variance with them for low ones. So is the experiment.

(3)   The flutter speed approaches zero as the two natural frequencies of the system merge. This correlates with the familiar tendency of a wing to exhibit an acute reduction in stability for unity frequency ratio.

(4)   Flutter onset can be delayed by raising the frequency of the high mode. Care should be taken, however, if the bending mode is the high-frequency mode. Since raising the stiffness in a mode gradually suppresses it, such a procedure would render the wing dominantly torsional. In this case, the nonstationary component of the aerodynamics is known to play a major role in the flutter process and the simplified bending-torsion flutter model consequently breaks down.

(5)   For a wing whose aerodynamic center lies forward of the center of mass, the flutter and divergence speed coalesce at their common end-point if the natural frequencies of the system are well separated.

V. THE EFFECT OF ENERGY DISSIPATION

The influence of damping on system stability is a subject of much question and controversy. The following discussion serves to present new aspects toward solving this issue, as well as to illustrate the intricacies involved.

In the first step we analyze the system by considering only structural damping while still ignoring aerodynamic energy dissipation. From equation (8) we obtain the corresponding characteristic polynomial by discarding damping of aerodynamic origin. We obtain

$$\frac{s^2 + 2\sigma_1 s + \omega_1^2 \left(1 - \dfrac{\overline{X}_E/\overline{X}_P}{}\right)}{s^4 + 2(\sigma_1 + \sigma_2) s^3 + (\omega_1^2 + \omega_2^2 + 4\sigma_1\sigma_2) s^2 + 2(\sigma_1\omega_2^2 + \sigma_2\omega_1^2) s + (\omega_1^2 \omega_2^2 - k_{12}k_{21})} = -\frac{1}{K} \cdot (26)$$

The expression still appears in the standard form which can be handled by the root locus method. Now the poles of the transfer function represent the damped coupled frequencies of the system. Their distance to the left of the imaginary axis is approximately given by their corresponding decay rates σ_1 and σ_2. The zeros of the transfer function are also lying in the left half plane, their distance from the imaginary axis being approximately equal to the decay rate σ_1 of the bending mode. An illustration of how flutter instability evolves in the presence of structural damping is provided in Figures 9-11 for the three basic flutter modes identified previously in the undamped system. A qualitative evaluation of the resulting change in the root locus pattern is afforded by the force analogy and the rules of the root locus method concerning departure and arrival angles at the poles and zeros, respectively. As can be seen, flutter onset is in general no longer associated with frequency coalescence when the system is damped. Under certain circumstances, however, the roots can still "meet" in the left half plane and then separate and become unstable. Examining the behavior pattern of the root loci, one discovers a rather interesting phenomenon: As a direct result of the closeness of the pole-zero constellation to the imaginary axis, the system can exhibit an extreme sensitivity toward variations of the damping parameters. Under certain conditions, minute variations of these parameters will result in drastic changes of the flutter frequency and also of the flutter speed. It can, for instance, readily be shown by applying the departure angle rule of the root locus method and intuitively understood from its force analogy that the introduction of an infinitesimal amount of damping in only one mode causes the flutter speed to drop to zero. Theoretically, at least, it is possible to reduce the flutter speed to any desired fraction of the undamped flutter speed by introducing a proper ratio of infinitesimal small damping in both modes. As a rule, however, the flutter speed is less sensitive toward parameter variations than the flutter frequency. Since, in general, the root closest to the axis becomes unstable, the critical parameter dictating the stability behavior of a mode is its decay rate rather than its damping ratio. In the light of these circumstances, physical interpretations which try to explain the source of instability of such a sensitive system in terms of changes in mode shapes, phase shifting or energy transfer between modes seem to be rather artificial and can even be misleading when applied to a particular case.

While the inclusion of structural damping still preserves the standard form of the characteristic polynomial suitable for the root locus method, this is no longer true for the aerodynamic energy dissipation. It not only causes the zeros of the transfer function to depend on the airspeed, but also introduces a new zero on the real axis. Evaluation of system stability in this case is more complicated and requires a familiarity with the root locus method which is beyond the scope of the present discussion. One can show, for instance, that a zero on the negative real axis would effectively cause the root loci to turn counterclockwise in the upper half plane and clockwise in the lower half plane. Hence, aerodynamic damping could effectively enhance system stability for the configuration depicted in Figure 9 (a) but reduce it for the configuration of Figure 9 (b). It should be emphasized, however, that the root locus method in this case can give at best qualitative results which might be useful for interpreting parametric studies.

As can be readily concluded from the above, the introduction of quasi-steady aerodynamics essentially destroys the usefulness of the root-locus method for obtaining quantitative answers. The method becomes even less helpful if one tries to incorporate more general unsteady aerodynamics, which then becomes a complicated function of the reduced frequency. As a consequence the gain K of the root locus method would also become a function of the reduced frequency. To obtain at least a qualitative impression of how a (constant) complex gain K would affect the pattern of the root loci, the flutter mode A-1 was taken as an example and its root loci constructed, assuming a phase lag of 20° which is approximately the maximum phase lag encountered in the Theodorsen analysis (Fig. 12). According to the rules of conformal mapping, a phase lag turns each segment of the root loci in the clockwise direction. As a consequence the root loci are no longer symmetric to the real axis and the systems has, in general, four distinct aeroelastic modes. On this basis one could infer that complex aerodynamics should generally have a destabilizing effect on the system.

VI. CONCLUSIONS

The root locus method furnishes a convenient tool for analyzing the aeroelastic stability behavior of a simplified bending-torsion flutter model and promotes an intuitive physical understanding of the flutter mechanism in terms of aerodynamic feedback coupling. Its usefulness is kept intact when structural damping is introduced into the system. As a consequence the method also provides a lucid explanation of the effects of energy dissipation on system stability and reveals the extreme sensitivity of the stability behavior with respect to damping parameter variations. The latter phenomenon is intrinsic to any system whose pole-zero constellation is close to the imaginary axis of the complex plane.

Extensions of the root locus method to systems involving many degrees of freedom are straight forward as long as the analysis is restricted to static aerodynamics. Such extensions could serve the purpose of isolating potentially dangerous flutter modes which would thereafter be subjected to a more accurate flutter analysis.

Inclusion of aerodynamic energy dissipation and unsteady aerodynamics renders the root locus method impractical for a quantitative stability analysis but still supplies qualitative statements about the stability behavior of the system that could be used as guidelines in preliminary design studies. Modifications of the root locus method involving an iterative process on a graphical basis could, of course, be developed in order to arrive at quantitative results. It is believed, however, that such a graphical technique could not compete with any of the existing digital flutter analyses in terms of accuracy, speed or other expenditures.
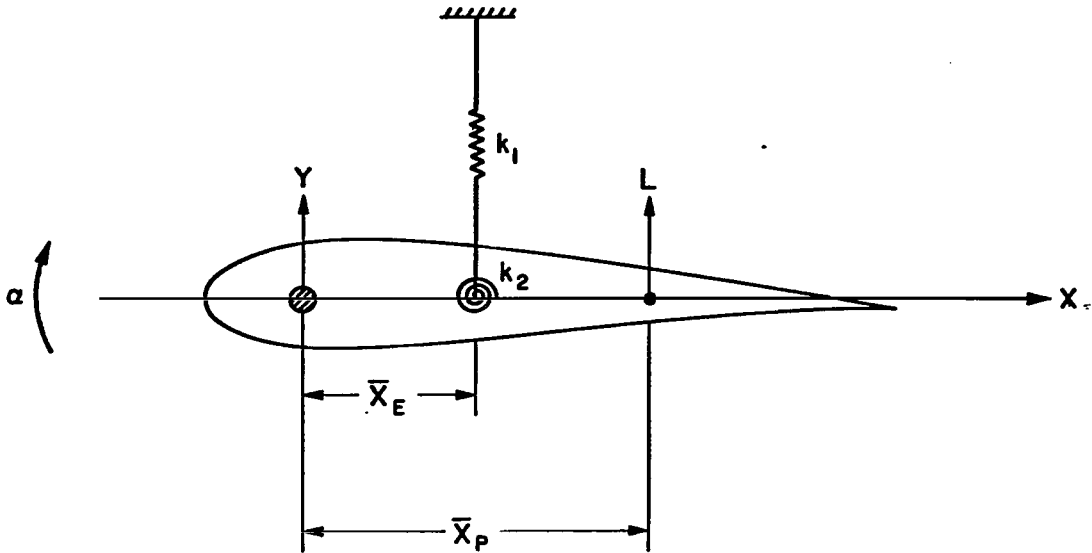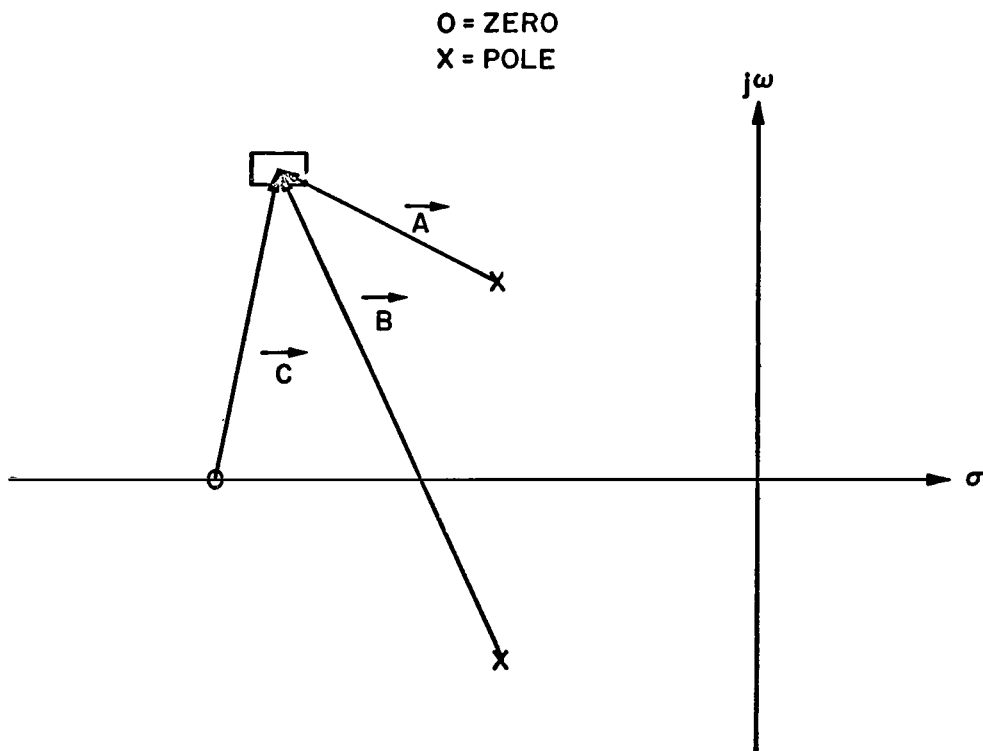
FIGURE 1. BENDING-TORSION FLUTTER MODEL

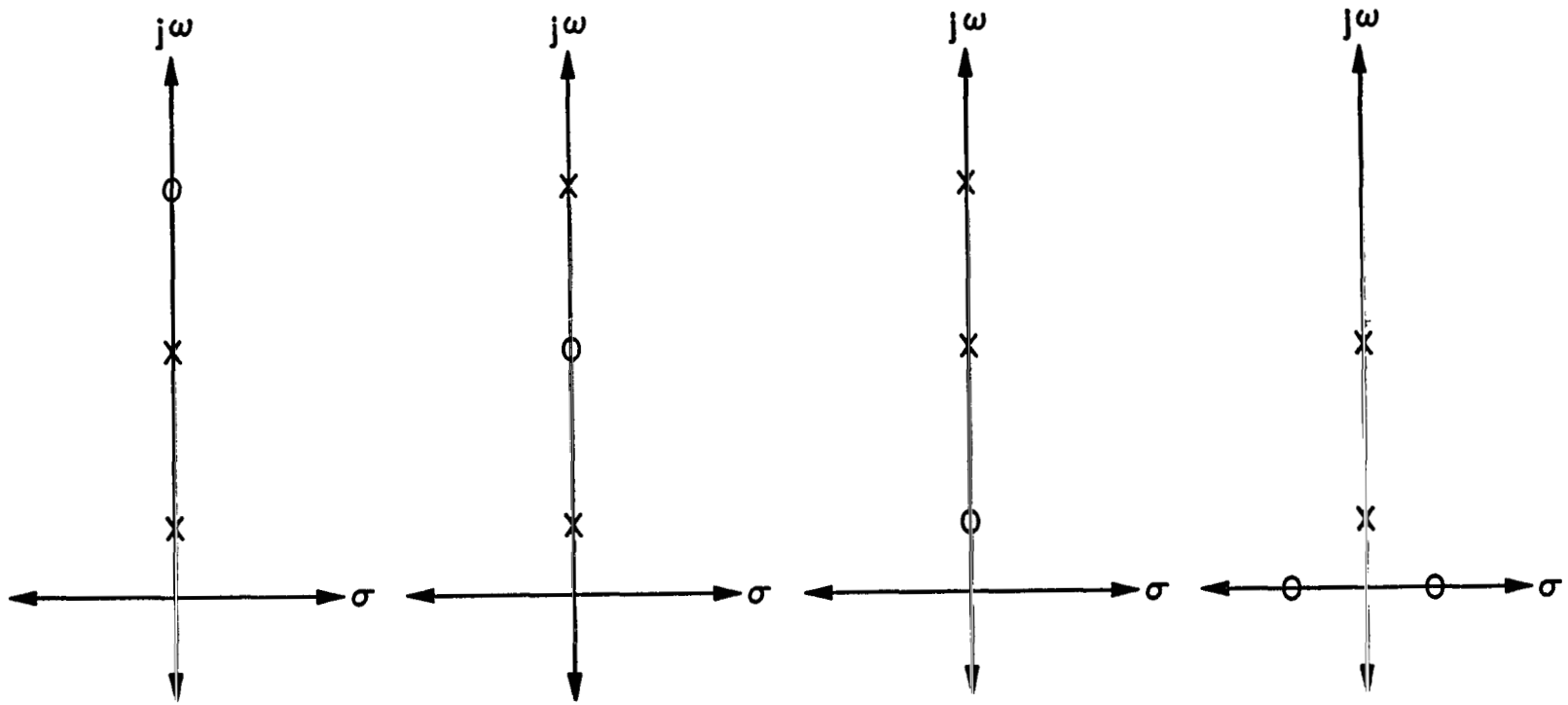O = ZERO
X = POLE

FIGURE 2. VECTOR REPRESENTATION OF TRANSFER FUNCTION G(S)

13

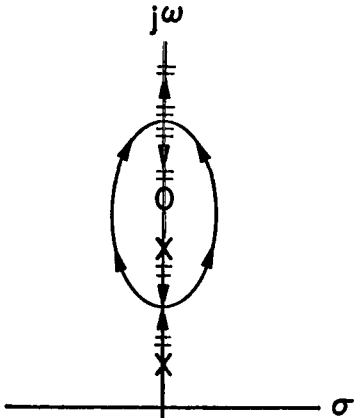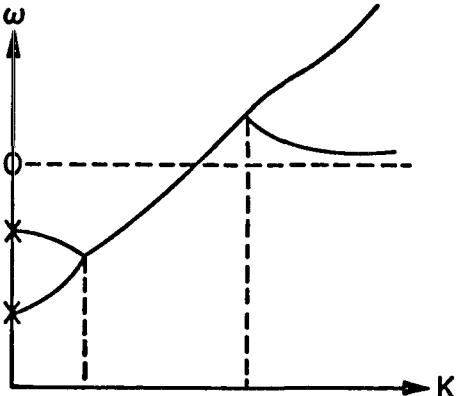FIGURE 3. BASIC POLE – ZERO CONSTELLATIONS (UPPER HALF – PLANE)
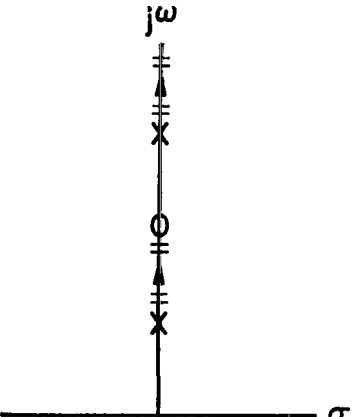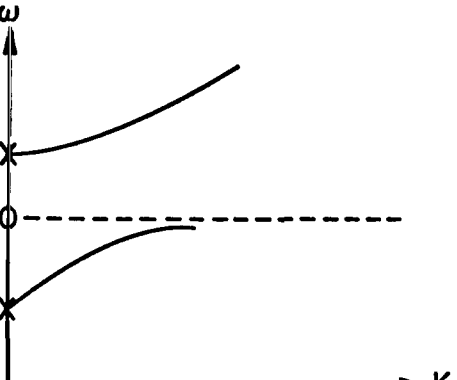
PARAMETER CONDITIONS	ROOT LOCUS	FREQUENCY CHARACTERISTICS
$\omega_2 > \omega_1$ $\overline{X}_E < \overline{X}_P \left[1 - \left(\dfrac{\omega_2}{\omega_1} \right)^2 \right]$ $\omega_2 < \omega_1$ $\overline{X}_E < 0$	CASE A1	FLUTTER FLUTTER
$\omega_2 > \omega_1$ $\overline{X}_P \left[1 - \left(\dfrac{\omega_2}{\omega_1} \right)^2 \right] < \overline{X}_E < 0$ $\omega_2 < \omega_1$ $0 < \overline{X}_E < \overline{X}_P \left[1 - \left(\dfrac{\omega_2}{\omega_1} \right)^2 \right]$	CASE A2	STABLE

FIGURE 4a. AEROELASTIC BEHAVIOR OF BENDING – TORSION MODEL

A: $\bar{X}_P > 0$
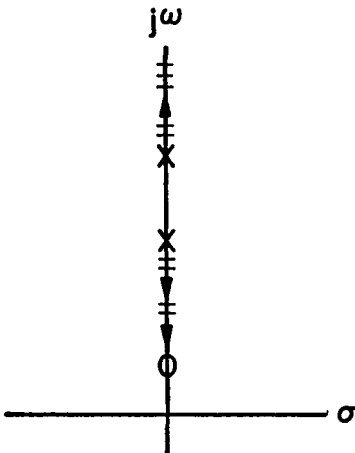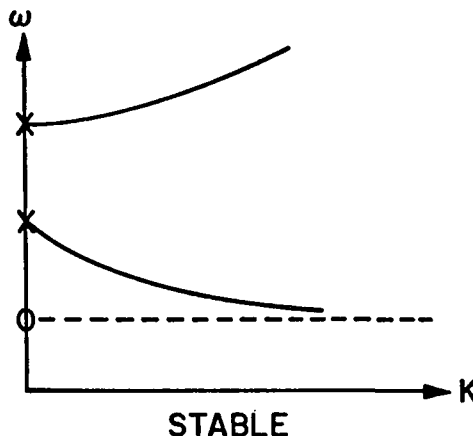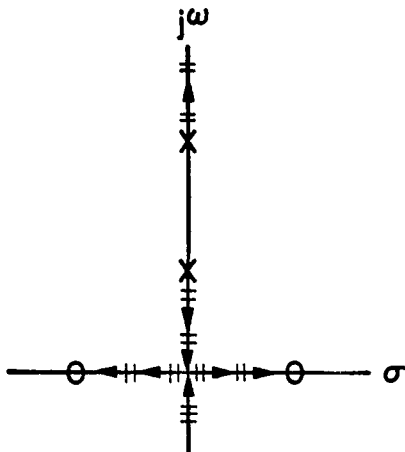
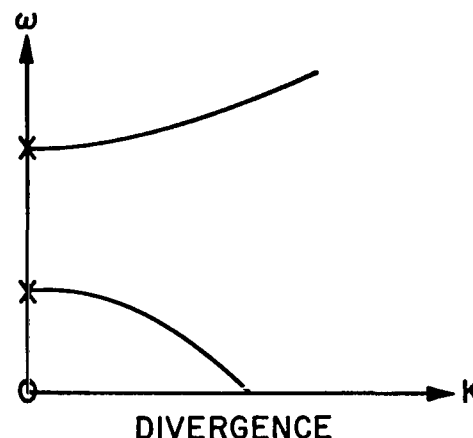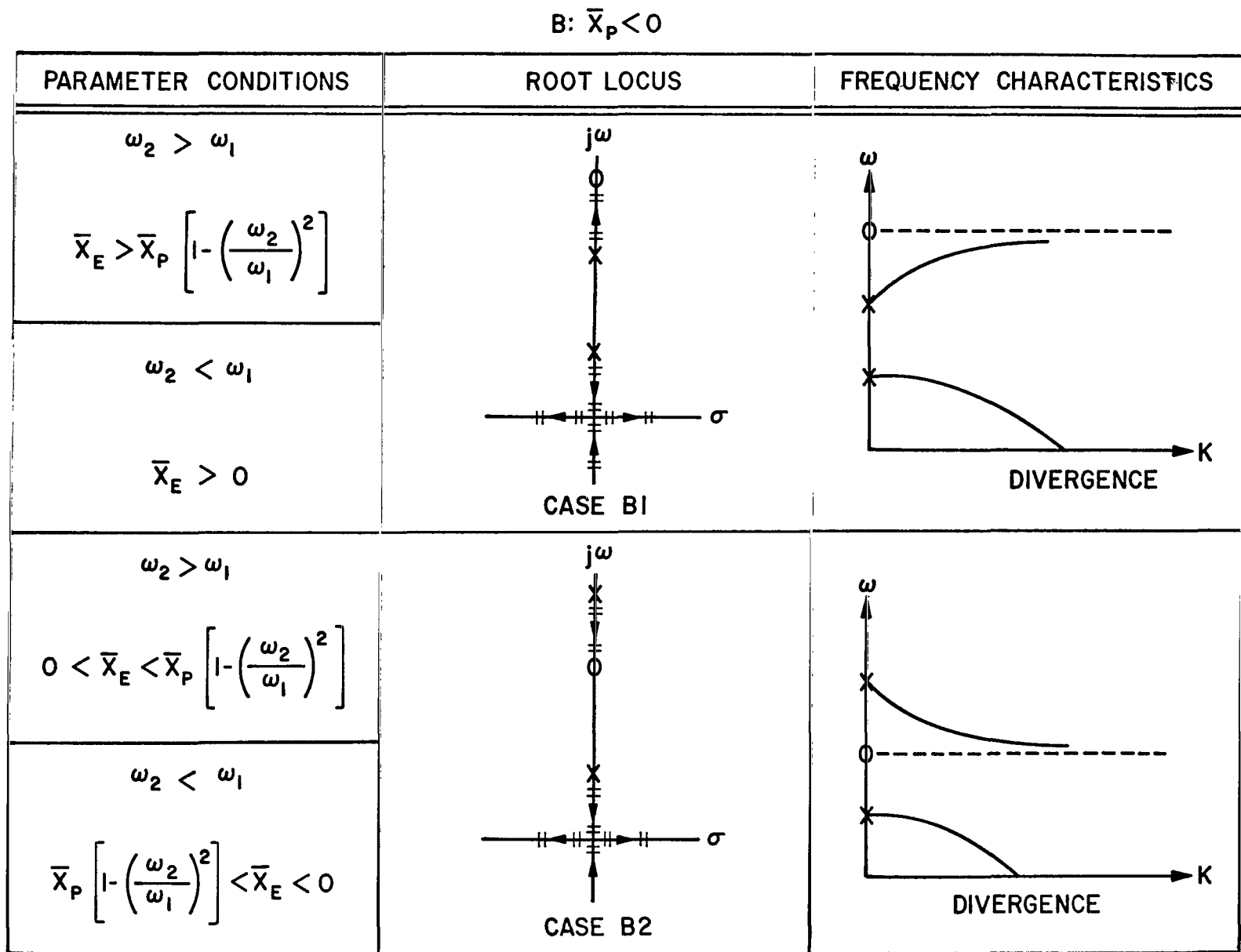| PARAMETER CONDITIONS	ROOT LOCUS	FREQUENCY CHARACTERISTICS
$\omega_2 > \omega_1$ $0 < \bar{X}_E < \bar{X}_P$ $\omega_2 < \omega_1$ $\bar{X}_P\left[1 - \left(\dfrac{\omega_2}{\omega_1}\right)^2\right] < \bar{X}_E < \bar{X}_P$	CASE A3	STABLE
$\omega_2 > \omega_1$ $\bar{X}_E > \bar{X}_P$ $\omega_2 < \omega_1$ $\bar{X}_E > \bar{X}_P$	CASE A4	DIVERGENCE

FIGURE 4b. AEROELASTIC BEHAVIOR OF BENDING – TORSION MODEL

PARAMETER CONDITIONS	ROOT LOCUS	FREQUENCY CHARACTERISTICS
$\omega_2 > \omega_1$ $$\overline{X}_E > \overline{X}_P \left[1 - \left(\frac{\omega_2}{\omega_1} \right)^2 \right]$$ $\omega_2 < \omega_1$ $\overline{X}_E > 0$	CASE B1	DIVERGENCE
$\omega_2 > \omega_1$ $$0 < \overline{X}_E < \overline{X}_P \left[1 - \left(\frac{\omega_2}{\omega_1} \right)^2 \right]$$ $\omega_2 < \omega_1$ $$\overline{X}_P \left[1 - \left(\frac{\omega_2}{\omega_1} \right)^2 \right] < \overline{X}_E < 0$$	CASE B2	DIVERGENCE

FIGURE 5a. AEROELASTIC BEHAVIOR OF BENDING – TORSION MODEL

B: $X_P < 0$
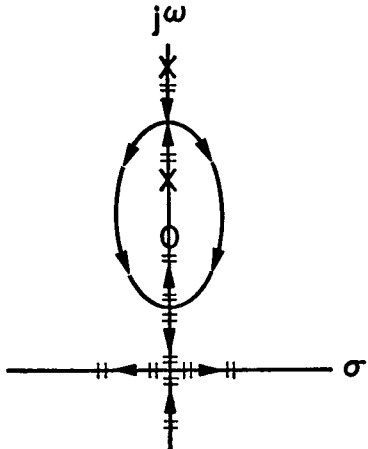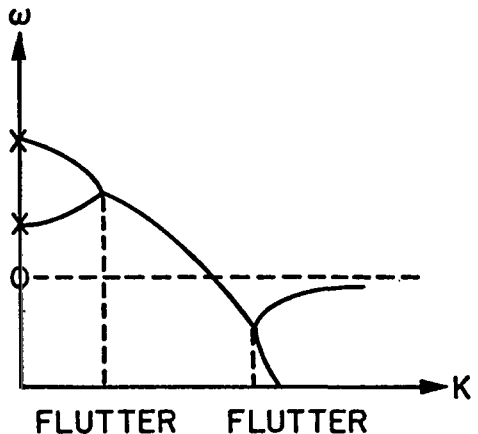
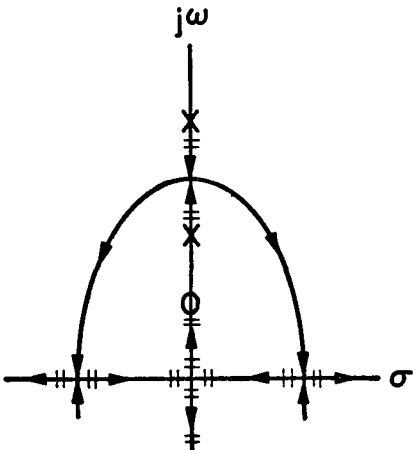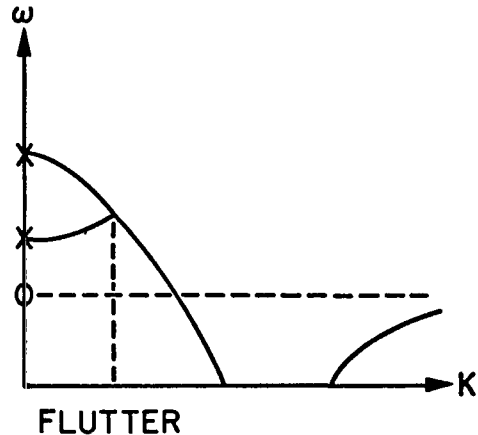| PARAMETER CONDITIONS	ROOT LOCUS	FREQUENCY CHARACTERISTICS
$\omega_2 > \omega_1$ $\overline{X}_P \dfrac{\omega_1{}^2}{\omega_1{}^2 + \omega_2{}^2} < \overline{X}_E < 0$ $\omega_2 < \omega_1$ $\overline{X}_P \dfrac{\omega_1{}^2}{\omega_1{}^2 + \omega_2{}^2} < \overline{X}_E < \overline{X}_P \left[1 - \left(\dfrac{\omega_2{}^2}{\omega_1{}^2} \right) \right]$	CASE B3a	FLUTTER FLUTTER
$\omega_2 > \omega_1$ $\overline{X}_P < \overline{X}_E < \overline{X}_P \dfrac{\omega_1{}^2}{\omega_2{}^2 + \omega_1{}^2}$ $\omega_2 < \omega_1$ $\overline{X}_P < \overline{X}_E < \overline{X}_P \dfrac{\omega_1{}^2}{\omega_2{}^2 + \omega_1{}^2}$	CASE B3b	FLUTTER

FIGURE 5b. AEROELASTIC BEHAVIOR OF BENDING – TORSION MODEL

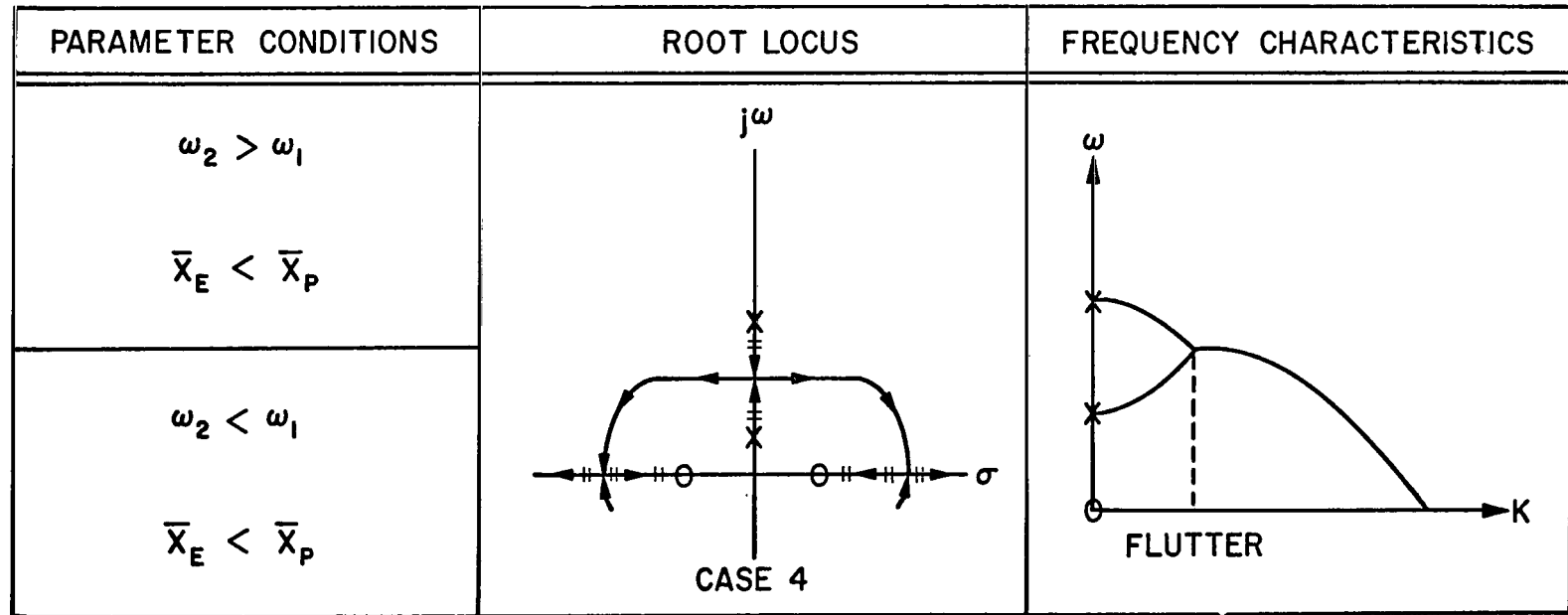| PARAMETER CONDITIONS	ROOT LOCUS	FREQUENCY CHARACTERISTICS
$\omega_2 > \omega_1$ $\overline{X}_E < \overline{X}_P$		
$\omega_2 < \omega_1$ $\overline{X}_E < \overline{X}_P$	CASE 4	FLUTTER

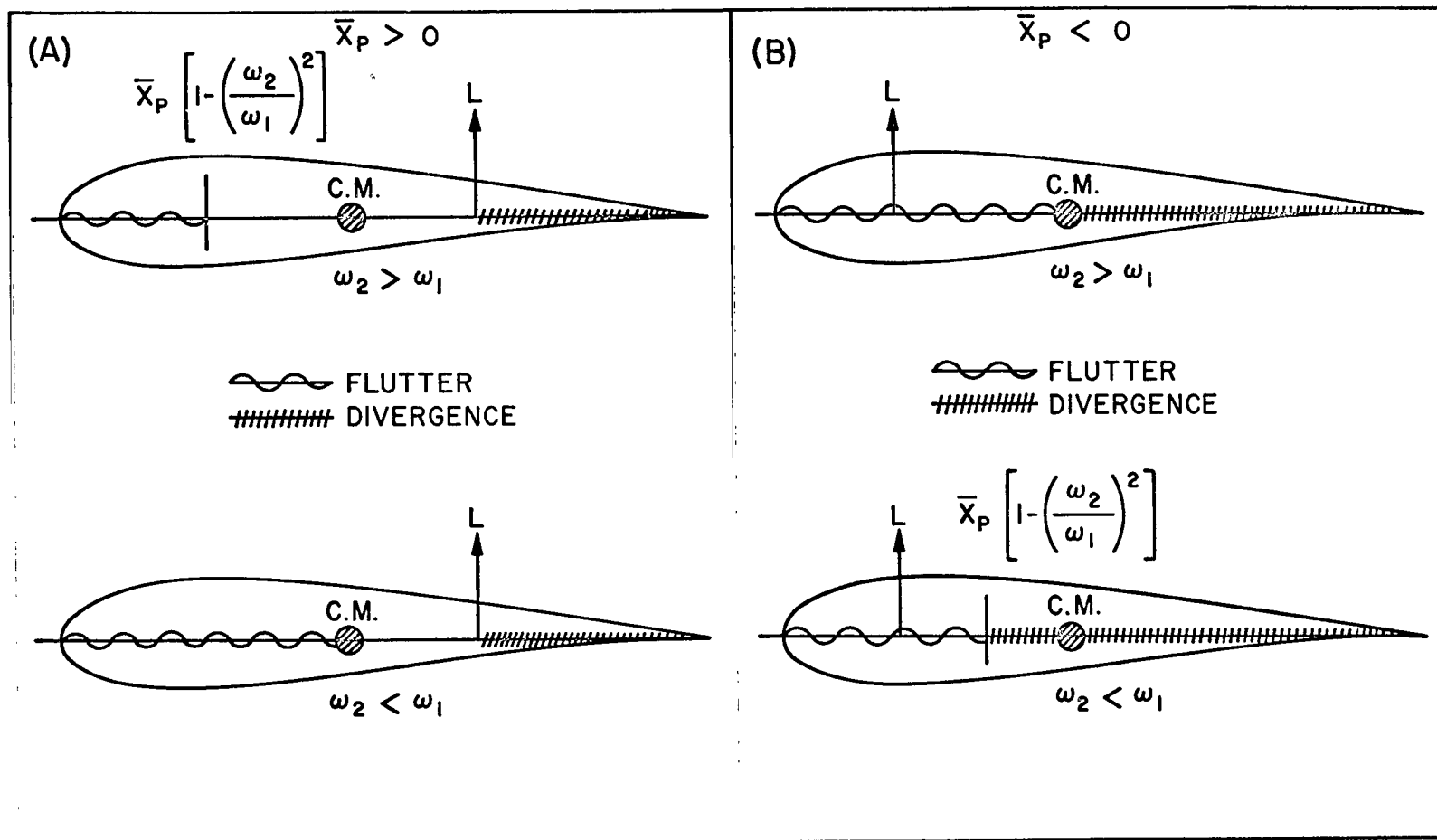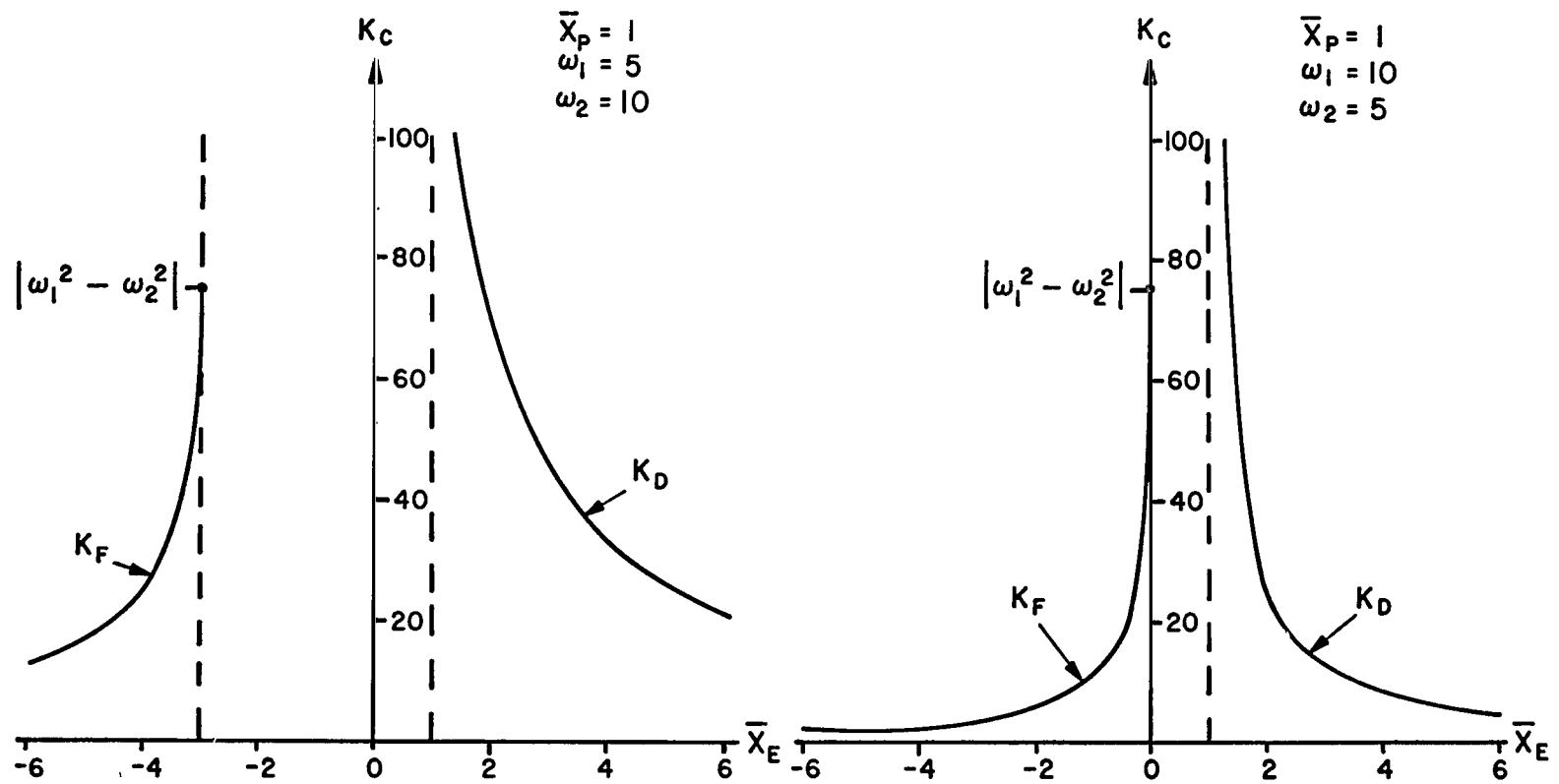FIGURE 5c. AEROELASTIC BEHAVIOR OF BENDING – TORSION MODEL

FIGURE 6. AEROELASTIC STABILITY CRITERIA

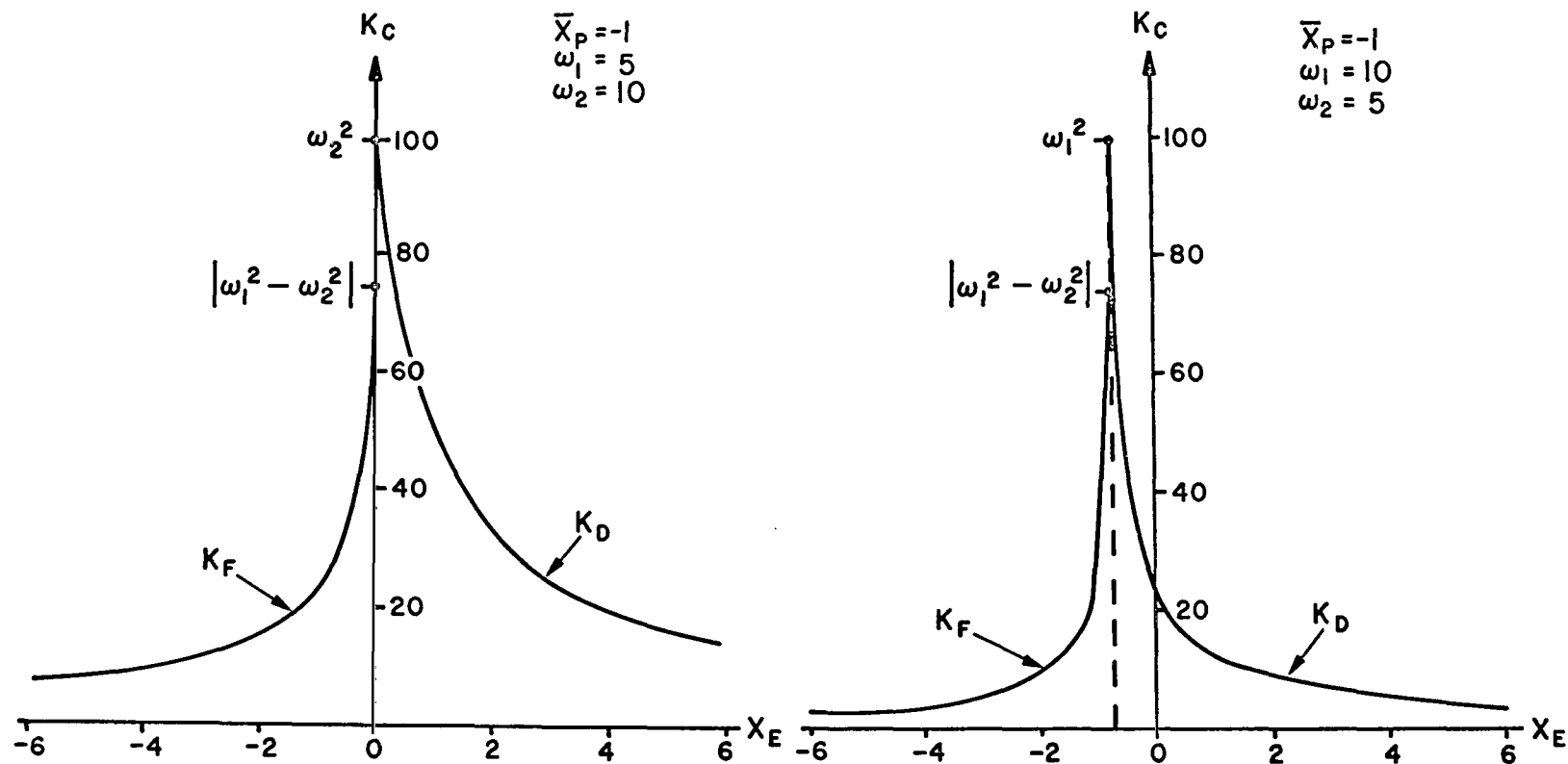FIGURE 7. CRITICAL GAIN VERSUS LOCATION OF ELASTIC AXIS

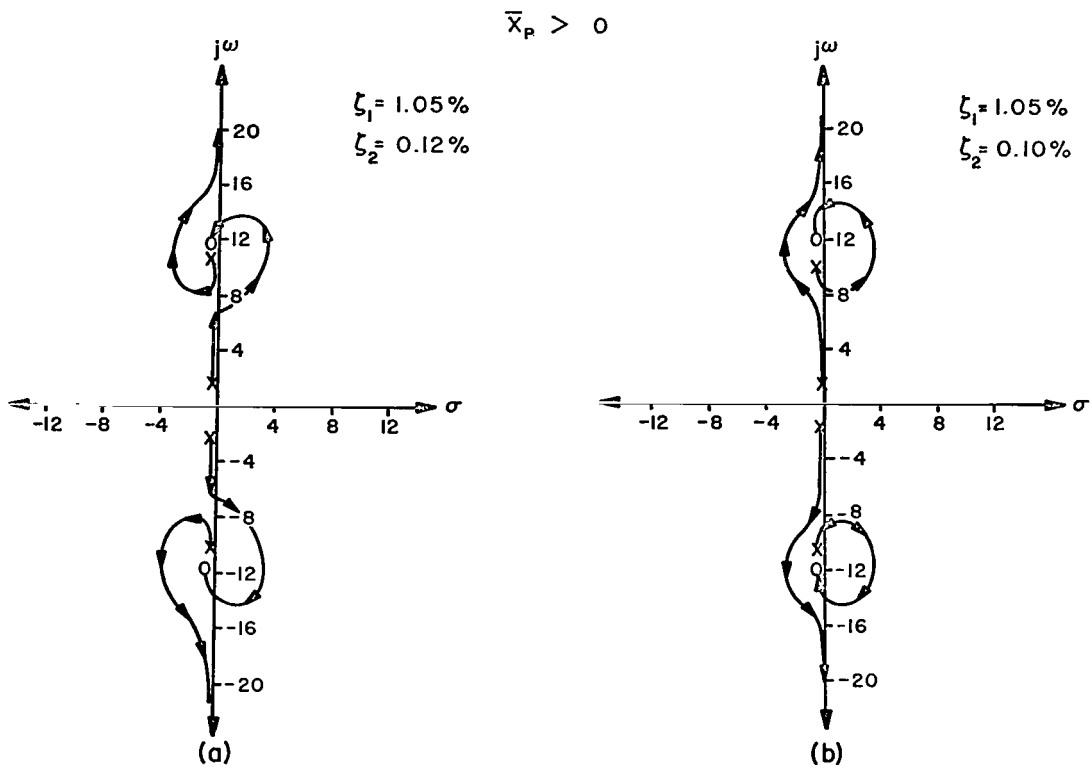FIGURE 8.   CRITICAL GAIN VERSUS LOCATION OF ELASTIC AXIS

$$\overline{X}_P > 0$$

(a)

$\zeta_1 = 1.05\%$
$\zeta_2 = 0.12\%$

(b)

$\zeta_1 = 1.05\%$
$\zeta_2 = 0.10\%$

FIGURE 9. EFFECT OF STRUCTURAL DAMPING ON FLUTTER MODE A1

$$\overline{X}_P < 0$$

(a)

$\zeta_1 = 0.6\%$
$\zeta_2 = 0.35\%$

(b)

$\zeta_1 = 0.6\%$
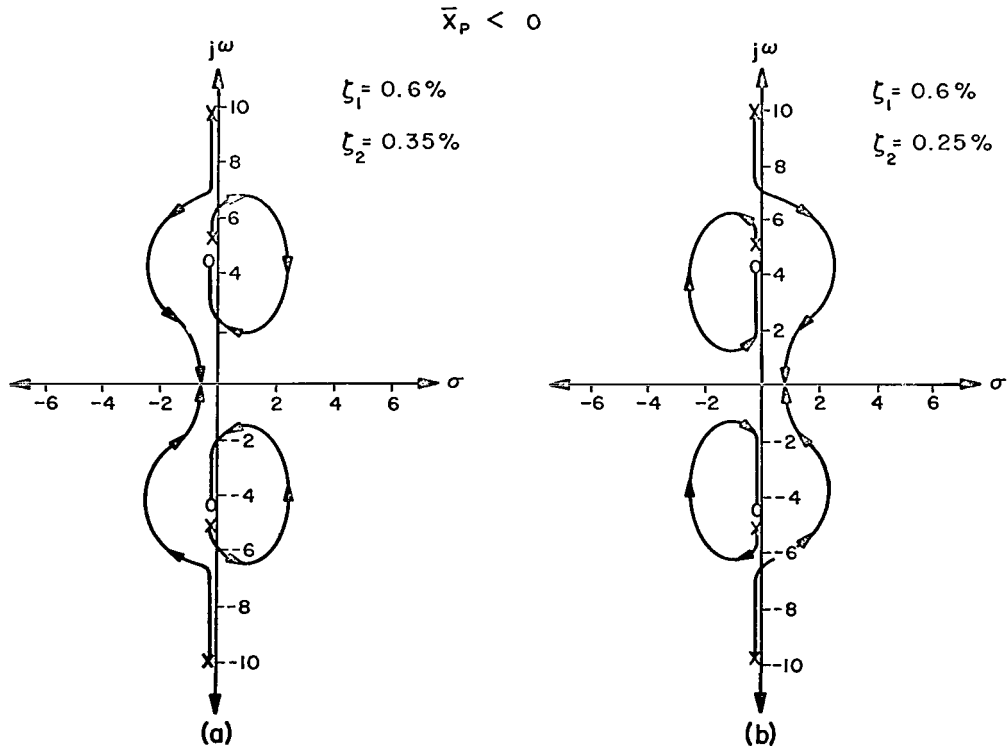$\zeta_2 = 0.25\%$

FIGURE 10. EFFECT OF STRUCTURAL DAMPING ON FLUTTER MODE B3a
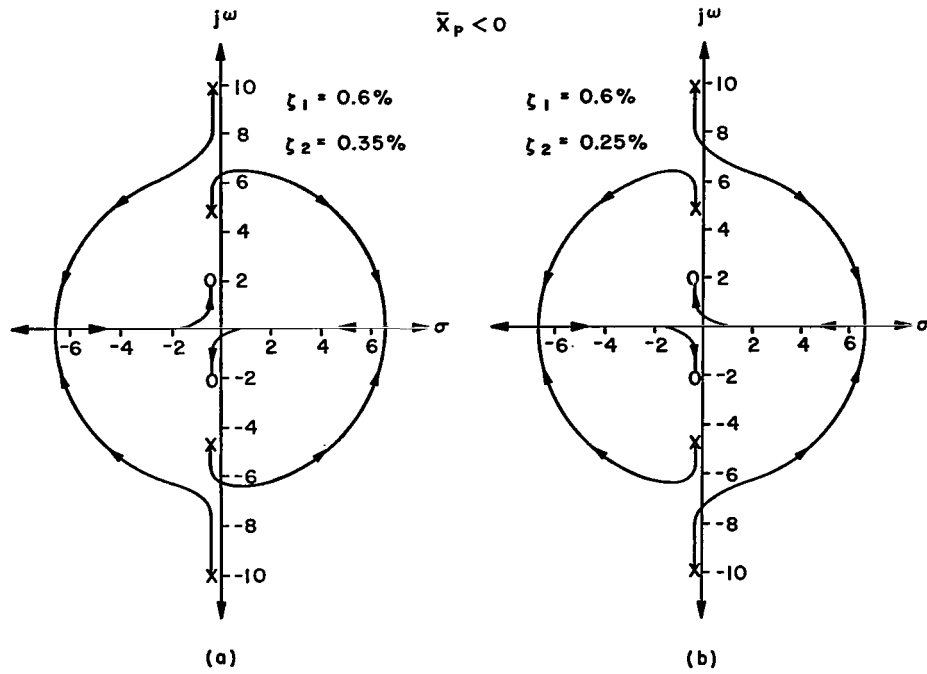
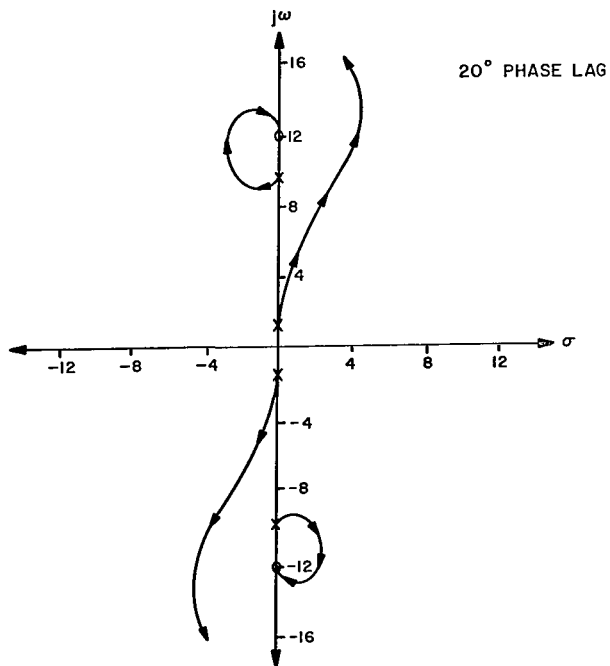FIGURE 11. EFFECT OF STRUCTURAL DAMPING ON FLUTTER MODE B3b

FIGURE 12. EFFECT OF COMPLEX GAIN ON FLUTTER MODE A1

24

REFERENCES

1. Karman von, T. and Biot, M. A., Mathematical Methods in Engineering, McGraw-Hill Book Co., New York, 1940.

2. Pines, S., "An Elementary Explanation of the Flutter Mechanism," Proceedings of Dynamics and Aeroelasticity Meeting, I. A. S., New York, 1958, pp 52-59.

3. Zimmerman, N. H., "Elementary Static Aerodynamics Adds Significance and Scope in Flutter Analyses," AIA Symposium Proceedings on Structural Dynamics of High Speed Flight, 1961, pp 28-84.

4. Bollay, William, "Aerodynamic Stability and Automatic Control," The Fourteen Wright Brothers Lecture, Journal of the Aeronautical Sciences, Vol. 18, No. 9, September 1951.

5. Truxal, John G., Automatic Feedback Control System Synthesis, McGraw-Hill Book Co., New York, 1955.

6. Wojcik, Charles K., "Analytical Representation of the Root-Locus," Journal of Basic Engineering, March 1964.

7. Fung, Y. C., An Introduction to the Theory of Aeroelasticity, John Wiley and Sons, New York, 1955.

"The aeronautical and space activities of the United States shall be conducted so as to contribute . . . to the expansion of human knowledge of phenomena in the atmosphere and space. The Administration shall provide for the widest practicable and appropriate dissemination of information concerning its activities and the results thereof."

—NATIONAL AERONAUTICS AND SPACE ACT OF 1958

NASA SCIENTIFIC AND TECHNICAL PUBLICATIONS

TECHNICAL REPORTS: Scientific and technical information considered important, complete, and a lasting contribution to existing knowledge.

TECHNICAL NOTES: Information less broad in scope but nevertheless of importance as a contribution to existing knowledge.

TECHNICAL MEMORANDUMS: Information receiving limited distribution because of preliminary data, security classification, or other reasons.

CONTRACTOR REPORTS: Technical information generated in connection with a NASA contract or grant and released under NASA auspices.

TECHNICAL TRANSLATIONS: Information published in a foreign language considered to merit NASA distribution in English.

TECHNICAL REPRINTS: Information derived from NASA activities and initially published in the form of journal articles.

SPECIAL PUBLICATIONS: Information derived from or of value to NASA activities but not necessarily reporting the results of individual NASA-programmed scientific efforts. Publications include conference proceedings, monographs, data compilations, handbooks, sourcebooks, and special bibliographies.

Details on the availability of these publications may be obtained from:

SCIENTIFIC AND TECHNICAL INFORMATION DIVISION

NATIONAL AERONAUTICS AND SPACE ADMINISTRATION

Washington, D.C. 20546